Ain Shams Engineering Journal 14 (2023) 101950

Contents lists available at ScienceDirect

Ain Shams Engineering Journal

journal homepage: www.sciencedirect.com

Super twisting sliding mode-type 2 fuzzy MPPT control of solar PV system with parameter optimization under variable irradiance conditions

Korhan Kayisli

Gazi University, Faculty of Engineering, Department of Electrical and Electronic Engineering, 06570 Ankara, Turkey

ARTICLE INFO

Article history:
Received 26 March 2022
Revised 15 July 2022
Accepted 22 August 2022
Available online 06 September 2022

Keywords:
MPPT
Super twisting sliding mode
Type 2 fuzzy control
Robust control
Boost converter
Parameter optimization

ABSTRACT

The need for renewable energy sources is increasing while the use of non-environmentally energy sources is decreasing day by day. At this point, solar energy which is a great natural energy source comes to the fore. In this study, MPPT control is performed based on sliding mode control as a robust control method. A super-twisting sliding mode controller has been developed and type 2 fuzzy set has been adapted to the system to reduce the chattering problem. The developed MPPT control algorithm is applied to a solar PV system and tested under variable irradiance conditions. In addition, the parameters of super twisting sliding mode and type 2 fuzzy set are optimized. The efficiency of the proposed MPPT algorithm is presented with tables and graphics that contains sliding mode MPPT, super twisting sliding mode MPPT and super twisting sliding mode-type 2 fuzzy MPPT methods. The results show the MPPT efficiency of proposed system with a robust structure.

1. Introduction

Semiconductor-based materials are widely used to generate electrical energy from solar energy. However, the efficiency of these materials is around 15–16 % for polycrystalline solar panels, 18–22 % for monocrystalline solar panels, and 20–22 % for P and N polycrystalline silicon cells with current technology. The low efficiency of solar panels, the constantly changes in temperature and radiation level, push researchers to develop methods that will ensure maximum use of the obtained power. At this point, maximum power point tracking (MPPT) techniques developed for the maximum power point are gaining more importance. While many studies have been carried out on this subject in recent years, the prominent MPPT techniques are perturb & observe (P&O), incremental conductance (IC), constant voltage (CV) and open-circuit voltage (OCV). There are many researches about MPPT techniques have been performed for the solar photovoltaic (PV) panel efficiencies. Especially P&O and IC algorithms are preferred for MPPT applications. For energy maximizing of solar PV systems, traditional P&O method is used in some studies [1–2]. Also modified and improved P&O MPPT algorithms are applied to PV systems for drift avoidance [3], higher efficiency [4], more robust control against rapidly varying weather conditions [5–10]. Another solution to enhance the efficiency performance, variable step size P&O MPPT is chosen in some studies [11–14]. In the literature, too many modified versions of P&O technique have been researched and implemented to improve the performance of classical method, more fast dynamic response and more robustness. Parameter uncertainties, variable weather conditions and load changes force the control method and, sometimes it can eliminate stability, durability and controllability. Sliding mode control (SMC) is well known control algorithm that provide robustness to the system and it can be a very useful method especially for non-linear systems. While some researchers have tried adapting the SMC to the P&O method through these control features [15], in another study, SMC have been used to control the current of converter [16]. Another preferred method to improve the performance of the P&O method is to gain an adaptive feature to this method. For this purpose, in one study, the grey-wolf method [17] is used, and in a few other studies, the particle swarm optimization (PSO) method for parameters and voltage-scanning based MPPT are explored [18–21]. Another widely used method is the incremental conductance (IC) method. The IC algorithm is based on the compar-

Peer review under responsibility of Ain Shams University.
E-mail: korhankayisli@gmail.com

Production and hosting by Elsevier

https://doi.org/10.1016/j.asej.2022.101950
2090-4479/

ison of the PV panel' conductivity and incremental conductivity. Accordingly, the voltage of the panel is increased or decreased to obtain maximum power from the PV panel. Most studies to demonstrate the performance of IC method have been compared with the P&O method [22–32]. Other study has preferred to compare the performance of the IC method with P&O, SMC and fuzzy control (FC) [33]. Additionally, FC method have been used to improve the performance of P&O method [34–38]. The used methods are not limited with the mentioned methods. Genetic algorithm based neural controller (GA-ANN) as another intelligent control algorithm appears to improve the performance of P&O method [39–40]. Also, fractional open circuit voltage (OCV) technique is adapted to P&O method and obtained a hybrid MPPT algorithm in another study [41]. In addition to these studies about control algorithms and their development, the use of different dc-dc converter topologies is among the studies about MPPT. Generally, boost dc-dc converter circuit is used because of its simple structure, low cost and convenient. Moreover, buck converter and buck-boost converter [42] and Cuk converter [43–45] have been implemented and used for MPPT applications on PV panels. In some studies, three-diode model of two commercial PV modules are used and nine important parameters have been obtained by using equilibrium optimizer algorithm, artificial electric field algorithm, transient search optimization algorithm and Harris Hawk optimization algorithm [60–63]. Also, another study related with parameter optimization of controllers by using Salp Swarm algorithm to enhance the low voltage ride through of grid-connected PV systems [64]. A fractional-order SMC based on a two-hidden-layer recurrent neural network and a fuzzy double hidden layer recurrent neural network is proposed for a single-phase shunt active power filter [65–66]. A fractional controller based on the terminal SMC and a recurrent Chebyshev fuzzy neural network using a self-evolving mechanism is designed to tracking control of trajectories [67].

In this study, after the reviewing the used and researched MPPT methods, it is aimed to increase the efficiency and robustness. For this aim, the SMC method was examined and it is desired to benefit from the robustness of this method with improving efficiency of MPPT application. Generally, many control algorithms have their own advantages and disadvantages. The chattering problem is one of the disadvantages of the SMC method in steady state. Using the saturation function (sat(.)) instead of the signum (sign(.)) function is one of the methods used to reduce and eliminate the chattering problem [46–47]. Another approach is to adapt the FC to the SMC and FC can be used in several different ways. At this point, using FC instead of sign or sat functions is one of the approaches [48–49]. It is possible to limit the chattering problem in steady state with FC. In this study, a robust control algorithm is used, which is minimally affected by parameter changes (irradiation variation). In this respect, the success of SMC is known by everyone. Firstly, in order to minimize the chattering problem, which is one of the disadvantages of this method, the super twisting-SMC (STSMC) algorithm was designed. Type 2 Fuzzy (T2FC) is adapted to the STSMC algorithm in order to minimize the variations in voltage, current, dc-dc converter output voltage and efficiency. The Lyapunov stability analysis is performed to prove the stability of proposed controller.

For this aim, Classical SMC and high order SMC methods such as twisting-SMC (TSMC), STSMC can be used. FC has also two options as classical (type 1) FC and T2FC. For MPPT application on PV systems, SMC based MPPT, STSMC based MPPT, and STSMC T2FC based MPPT (STSMC-T2FC) methods are developed and implemented to the same PV system.

Firstly, PV system and dc-dc boost converter circuit are modelled with using MATLAB/Simulink. Secondly, the proposed three algorithms about SMC and FC methods are implemented on the proposed PV system. The performances of the MPPT algorithms under variable irradiance conditions are shown with comparative graphics and tables which contains performance parameters.

2. Modelling of the system

2.1. Model of PV module

The International Renewable Energy Agency predicts that approximately 85 % of the energy produced in 2050 will be met from renewable energy. Additionally, it is aimed that the energy produced from sun will be 20 % of the total energy in 2050 and increases the importance of electricity generation from solar energy. One of the methods used to obtain electrical energy from solar energy is the use of semiconductor-based PV array. PV solar cells can be characterized as a system containing semiconductor materials such as Silicon, Gallium, Arsenide, Cadmium Telluride or Copper Indium Diselenide, which directly converts sunlight (photons) on to itself. There are two commonly used methods to model of PV cells such as single diode model and two diode model [50,51]. The researches show that the efficiencies of both models are very close at 25^{O}C temperature condition. A single diode model is preferred in this study and shown in Fig. 1.

The mathematical model which includes current–voltage relation can be easily obtained from the previous studies. In this circuit, current of the PV cell is obtained by using the Eq. (1) from basic circuit laws.

$$I_{PV} = I_{Ph} - I_D - I_{Rp} \tag{1}$$

Also, current of an ideal diode I_D can be modelled with Shockley Equation and is given in Eq. (2).

$$I_D = I_s\left[\exp\left(\frac{V_{PV} + I_{PV}R_S}{\eta V_T}\right) - 1\right] \tag{2}$$

Thermal voltage V_T is obtained by using Eq. (3).

$$V_T = kT_C/q \tag{3}$$

If Eqs. (1)–(3) are used to get the main expression for the cell behavior, Eq. (4) is obtained and generally called as single diode cell model.

$$I_{PV} = I_{Ph} - I_D\left[\exp\left(\frac{V_{PV} + I_{PV}R_S}{\eta V_T}\right) - 1\right] - \frac{V_{PV} + I_{PV}R_S}{R_P} \tag{4}$$

For a diode array, the number of series N_S and parallel cell N_P numbers should be added to Eq. (4).

$$I_{PV} = N_P I_{Ph} - N_P I_D\left[\exp\left(\frac{V_{PV} + \frac{N_S}{N_P} I_{PV}R_S}{N_S \eta V_T}\right) - 1\right] - \frac{V_{PV} + \frac{N_S}{N_P} I_{PV}R_S}{\frac{N_S}{N_P}R_P} \tag{5}$$

With some assumptions, Eq.6 can be obtained.

$$I_{PV} = N_P I_{Ph} - N_P I_D\left[\exp\left(\frac{qV_{PV}}{N_S \eta V_T}\right) - 1\right] \tag{6}$$

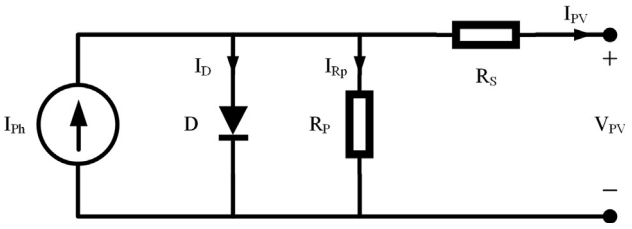

Fig. 1. Single diode model of PV cell.

When the PV panel is in short-circuit situation, V_{PV} = 0 and I_{PV} = $N_P I_{SC}$, also when the PV panel is in open-circuit situation, V_{PV} = $N_S V_{OC}$ and I_{PV} = 0. In these expressions, I_{SC} is short circuit current, V_{OC} is open circuit voltage of PV panel. If we arrange the Eq. (5) with these assumptions, the Eq. (7) can be obtained.

$$I_{PV} = N_P I_{SC} - N_P I_{SC}\left[\exp\left(\frac{V_{PV} + N_S V_{OC}}{N_S \eta V_T}\right)\right] \tag{7}$$

2.2. Model of DC-DC boost converter

There are many converter circuits that can be used in this structure. The boost dc-dc converter circuit, which is widely used, has been preferred because it is well known, easy to implement and has high efficiency. This converter works to convert the dc voltage applied to its input to a higher level. The used circuit of the boost dc-dc converter with an input filter capacitor C_{PV} is shown in Fig. 2.

The circuit is examined in two cases, depending on whether the switch (Q) is ON or OFF state. So, the characteristic equations of the inductor current (I_L) and the voltage of output capacitor (V_O) are obtained on Eqs. (8) and (9).

$$\frac{dI_L}{dt} = \frac{V_{PV} - V_O}{L} + \frac{V_O}{L}u \tag{8}$$

$$\frac{dV_O}{dt} = \left(-\frac{V_O}{RC_O} + \frac{I_L}{C_O}\right) - \frac{I_L}{C_O}u \tag{9}$$

By combining these equations, the state space equation of the dc-dc boost converter circuit is obtained in matrix form at Eq. (10) with assuming I_L = I_{PV}.

$$\frac{d}{dt}\begin{bmatrix} I_{PV} \\ V_O \end{bmatrix} = \begin{bmatrix} 0 & -1/L \\ 1/C_O & -1/RC_O \end{bmatrix}\begin{bmatrix} I_{PV} \\ V_O \end{bmatrix} + \begin{bmatrix} V_O/L \\ -I_{PV}/C_O \end{bmatrix}u + \begin{bmatrix} 1/L \\ 0 \end{bmatrix}V_{PV} \tag{10}$$

3. Second order SMC for MPPT

The SMC is often used as a robust controller in systems where nonlinear and parameter uncertainties exist. The chattering problem that occurs in the SMC method which is widely used in the control of DC-DC converters. This problem can be reduced with using variable switching frequency. But generally, the researchers prefer to use fixed switching frequency on microcontroller-based applications. There are some methods that can be used to overcome the chattering problem. At this situation, saturation function, fuzzy adaptation or high order SMC usage can be a solution. In this study, our aim is to get maximum power point with minimum chattering. MPPT is a technic that means maximum power point tracker. Also, second order SMC based on the super twisting algorithm (STSMC) is preferred to get maximum power from PV panel with chattering minimization. In the literature, the presented studies show the enhanced chattering problem reduction of STSMC on MPPT control [52]. In this method, there is no need to the time derivations of the sliding variable and it saves the advantages of the classical SMC. The trajectories oscillate with twisting on the sliding surface instead of chattering.

There are two steps for developing of SMC. The first step is to design a sliding surface where the dc-dc converter behaves as desired. The second step is to design a control law so as to push and maintain the system on the sliding surface. When a sliding surface is chosen as S(x,t), it should be equal to zero and also its first derivation too.

$$S(x,t) = 0,\ \dot{S}(x,t) = 0 \tag{11}$$

Reaching and staying on the sliding surface of the system trajectories will provide us maximum power. With this aim, Eq. (12) can be used for sliding surface [52,53].

$$S(x,t) = \frac{\partial P_{PV}}{\partial V_{PV}} = V_{PV}\left(\frac{\partial I_{PV}}{\partial V_{PV}} + \frac{I_{PV}}{V_{PV}}\right) = 0 \tag{12}$$

The general control law contains two components as the STSMC term for non-linear control (u_{STSMC}) and the equivalent control term (u_{eq}) and, it is given in Eq. (13).

$$u = u_{STSMC} + u_{eq} \tag{13}$$

The control of the STSMC algorithm is shown in Eq. (14) [52].

$$u_{STSMC} = -\lambda_1 |S|^{1/2}\mathrm{sign}(S) - \lambda_2 \int \mathrm{sign}(S) \tag{14}$$

$$X = \begin{bmatrix} I_L \\ V_O \end{bmatrix} \tag{15}$$

$$\dot{X} = f(X) + g(X)u \tag{16}$$

$$f(X) = \begin{bmatrix} \frac{V_{PV} - V_O}{L} \\ \frac{I_{PV}}{C_O} - \frac{V_O}{RC_O} \end{bmatrix} g(X) = \begin{bmatrix} \frac{V_O}{L} \\ -\frac{I_{PV}}{C_O} \end{bmatrix} \tag{17}$$

$$\dot{S} = \left[\frac{\partial S}{\partial X}\right]^T \dot{X} = \left[\frac{\partial S}{\partial X}\right]^T (f(x) + g(x)u_{eq}) = 0 \tag{18}$$

$$u_{eq} = \frac{\left[\frac{\partial S}{\partial X}\right]^T f(X)}{\left[\frac{\partial S}{\partial X}\right]^T g(X)} = 1 - \frac{V_{PV}}{V_O} \tag{19}$$

By using Eqs. (15)–(18), u_{eq} is obtained as shown in Eq. (19). The next step is to prove the stability of the proposed control. The Lyapunov stability analysis is generally used for this purpose.

3.1. Lyapunov stability analysis

Lyapunov Stability analysis is a well-known method that can be used to analyze of a non-linear system' stability. This method use of a selected Lyapunov function V(x) acting with the dynamics of the system. The V(x) must be selected with the following properties which is shown in Eq. (20).

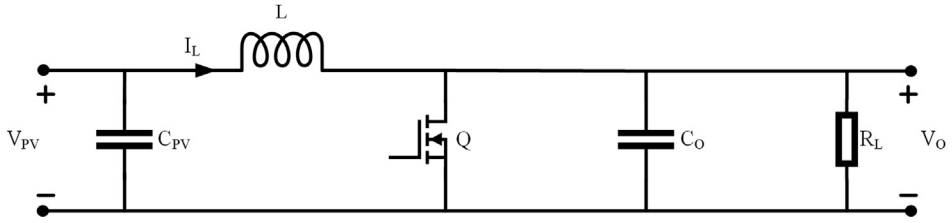

Fig. 2. The used boost dc-dc converter circuit.

$$\begin{cases} V(x) = 0 \text{ if and only if } x = 0 \\ V(x) > 0 \text{ if and only if } x \neq 0 \\ \dot{V}(x) = \nabla V.f(x) \leq 0 \text{ for all values o } x \neq 0 \end{cases} \quad \text{for asymptotic stability} \tag{20}$$

For the positive defined V(x) function depend on S(x,t) can be selected as Eq. (21).

$$V(x,t) = \frac{1}{2}(S(x,t))^2 \tag{21}$$

The first derivative of the proposed S(x,t) is obtained and shown in Eq. (22).

$$\dot{S} = \left[\frac{\partial S}{\partial X}\right]^T \dot{X} \tag{22}$$

$$\dot{S} = \left[\frac{\partial S}{\partial I_{PV}}\right]\left(-\frac{V_O}{L}(1-u) + \frac{V_{PV}}{L}\right) \tag{23}$$

The first term of the Eq. (23) is shown in Eq. (24).

$$\frac{\partial S}{\partial I_{PV}} = \frac{1}{V_{PV}} - \frac{I_{PV}}{V_{PV}^2}\frac{\partial V_{PV}}{\partial I_{PV}} + \frac{q}{N_S \eta V_T}\frac{\partial I_{PV}}{\partial V_{PV}}\frac{\partial V_{PV}}{\partial I_{PV}} \tag{24}$$

The first derivative of I_{PV} is defined as in Eq. (25).

$$\frac{\partial I_{PV}}{\partial V_{PV}} = -\frac{q}{N_S \eta V_T} I_D \exp\left(\frac{q}{N_S \eta V_T}\right) \tag{25}$$

Also, if the Eq. (6) can be arranged again, V_{PV} is obtained as in Eq. (26).

$$V_{PV} = \frac{N_S \eta V_T}{q} \ln\left(\frac{I_{PH} + I_D - I_{PV}}{I_D}\right) \tag{26}$$

The derivative of Eq. (25) is given in Eq. (27).

$$\frac{\partial V_{PV}}{\partial I_{PV}} = -\frac{N_S \eta V_T}{q} \ln\left(\frac{I_D}{I_{PH} + I_D - I_{PV}}\right) \tag{27}$$

After these operations, the sign of the Eq. (23) is obtained as positive $\frac{\partial S}{\partial I_{PV}} > 0$ and the sign of the second term is required. If the second term is arranged by using Eqs. (13) and (19), the final expression is obtained as Eq. (28).

$$\dot{X} = -\frac{V_O}{L}\left(1 - \left(1 - \frac{V_{PV}}{V_O}\right) - u_{STSMC}\right) + \frac{V_{PV}}{L} \tag{28}$$

$$S\dot{S} = S\left[\frac{\partial S}{\partial I_{PV}}\right]\frac{V_O}{L}\left(-\lambda_1 |S|^{1/2} \text{sign}(S) - \lambda_2 \int \text{sign}(S)\right) \tag{29}$$

The Eq. (29) show the stability that S and $\dot{S}$ always have opposite signs and provides the Lyapunov stability criteria. SMC [53], TSMC which stability analyzes have been performed on previous studies and STSMC structures can be given as with Eqs. (30), Eq. (31) and Eq. (32), respectively.

$$u_{SMC} = u_{eq} - \lambda_3 \text{sign}(S) \tag{30}$$

$$u_{TSMC} = u_{eq} - \lambda_4 \text{sign}(S) - \lambda_5 \text{sign}\left(\dot{S}\right) \tag{31}$$

$$u_{STSMC} = u_{eq} - \lambda_1 |S|^{1/2} \text{sign}(S) - \lambda_2 \int \text{sign}(S) \tag{32}$$

4. Fuzzy logic control

Fuzzy Logic and fuzzy set theory were first proposed by Prof. Lotfi A. Zadeh in 1965. This field has attracted the attention of many scientists and has been used in many applications. Fuzzy logic has been applied in many different fields such as process control, communication, business and medicine. However, studies in the field of fuzzy logic are concentrated in the field of control [54–55].

In Boolean Logic, an element is either an element of a set or it is not. Such sets are called as crisp sets. A crisp set for the age sample is shown in Fig. 3. In this example, persons between the ages of zero and thirty are defined as young, persons between the ages of thirty and fifty are defined as middle-aged, and persons over the age of fifty are defined as elderly.

Instead of crisp logic, sets are defined such as less hot, hot, very hot in fuzzy logic systems. Then, a membership degree in the range of [0 1] is calculated within the fuzzy sets for each input value and this situation creates a more appropriate logic in some applications. Fuzzy sets are represented by membership functions [54]. These membership functions can be defined as type-1 and type-2.

4.1. Type 2 fuzzy systems

The main problem of the classical SMC controller is the chattering problem. This is due to the use of the sign function, which directly affects the behavior in the steady state. The value range of the sign function is [-1,1]. Therefore, whether the value of the error is large or small changes only the sign of the output of the sign function and cannot adjust its size. In a previous study [48], good results were obtained experimentally by using the classical FC instead of the sign function. T2FC was preferred due to its two-dimensional band structure, increasing the sensitivity and aiming to increase the performance.

The type-2 fuzzy set was put forward by Zadeh as an extension of type-1 fuzzy set concept. If there is a problem in determining the degree of membership in the range of [0, 1], to use of type-2 fuzzy sets can be more effective [56]. Type-2 Fuzzy Logic Systems (T2FS) consists of fuzzy *If-Then* rules containing type-2 fuzzy sets. It can be said that uncertainty is not only limited to linguistic variables, but also a generalization of T1FS [55–58].

The general structure of T1FS and T2FS are shown in Fig. 4. When Fig. 4 is examined, it is seen that T2FS and T1FS are similar to each other. The major difference between them is that the defuzzification unit of T1FS is replaced by type reduction followed by defuzzification in T2FS [57–58].

The type2 membership functions of a T2FS represented with $\tilde{A}$ is denoted by $\mu_A(x,u)$ and it is expressed as in Eq. (33) ($x \in X$ and $u \in J_x \subseteq [0,1]$) [57–58].

$$\tilde{A} = \{(x,u), \mu_{\tilde{A}}(x,u) | \forall x \in X, \forall u \in J_x \subseteq [0,1]\} \tag{33}$$

Fig. 3. Crisp Set Example for Age.

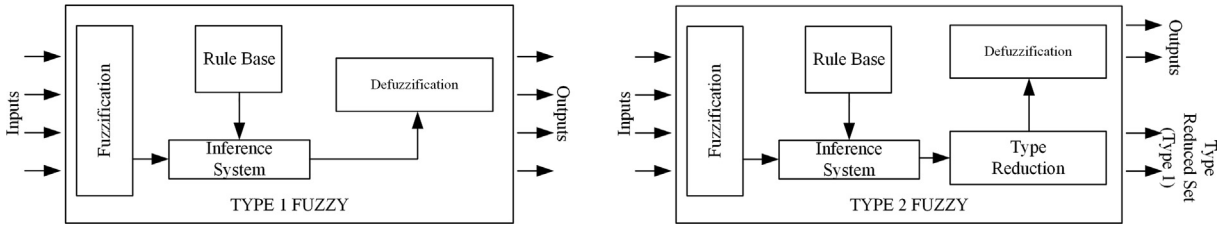

Fig. 4. Structure of Type 1 and Type 2 Fuzzy Sets.

In the Eq. (33), the membership function $\mu_{\tilde{A}}(x,u)$ is defined in [0,1]. Also, $\tilde{A}$ can be specified as in Eq. (34) [58–59].

$$\tilde{A} = \int_{x\in X}\int_{u\in J_x} \mu_{A^{\sim}}(x,u)/(x,u) J_x \subseteq [0,1] \tag{34}$$

The $(\int\int)$ is in Eq. (34) represents all acceptable $\times$ and u spaces. With $\forall u \in J_x \subseteq [0,1]$, J_x is the primary membership function of x. In addition, each primary membership value has a corresponding secondary membership value. The uncertainty in the primary membership functions of the T2FS ($\tilde{A}$) consists of a limited region called the uncertainty footprint (FOU). Mathematically, the FOU is the combination of all primary MFs. The MF of a general T2FS is three-dimensional, and a cross-section of a slice is shown in the Fig. 5. Only the boundary of the cross-section is used to define the MF of the set [57–58].

Since the T2FSs are difficult to understand and use, a T2FS called as interval T2FS has been proposed in literature [59].

4.2. Interval type 2 fuzzy systems

If all $\mu_{\tilde{A}}(x,u)$ are equal to 1 (one), then $\tilde{A}$ is called as interval Type 2 Fuzzy System (IT2FS). The Eq. (34) is determined as Eq. (35) for IT2FS [57–58].

$$\tilde{A} = \int_{x\in X}\int_{u\in J_x} 1/(x,u) J_x \rho \subseteq [0,1] \tag{35}$$

The MF of the IT2FS set is shown in the Figure. The third-dimension value for an IT2FS is the same everywhere. This means that the third dimension of IT2FS contains no new information. Therefore, the third dimension is neglected and only FOU is used to describe IT2FS.

As seen in Fig. 6, the MFs of IT2FS are combined with two type-1 membership functions as an upper membership function (UMF) and a lower membership function (LMF), which is the boundary for the FOU of T2FS $\tilde{A}$ is shown [57–58]. The most important difference between T1FS and T2FS is the use of type-2 MFs in T2FS. The structure of the rules in both fuzzy set is exactly the same. Rule structure of a T2FS with n inputs is given in Eq. (36) [57–58].

$$\text{r.Rule}: \text{If } x_1 = \tilde{A}_1^i,\ x_2 = \tilde{A}_2^i, \cdots, x_n = \tilde{A}_n^j, \text{ then } y = C^i \tag{36}$$

In Eq. (36), M represents the rules, j = 1, . . ., N, $x \in X$ and $y \in Y$. Also, this equation shows the type-2 relationship between input space X and output space Y of T2FS.

Fuzzy Inference Mechanism: The inference process in T2FS is very similar to T1FS. In the inference mechanism, the rules are combined and mapped the input T2FS to the output T2FS. For this matching process, it is necessary to calculate the *unions* and *intersections* of T2FS, as well as the combinations of type-2 relationships. Instead of *intersection* and *union* operations, *joining* and *meeting* operations are used in T2FS. *Joining* and *meeting* operations are used in secondary MFs [57–58]. C^j is j. result range set of the if-then rule as shown in Eq. (37).

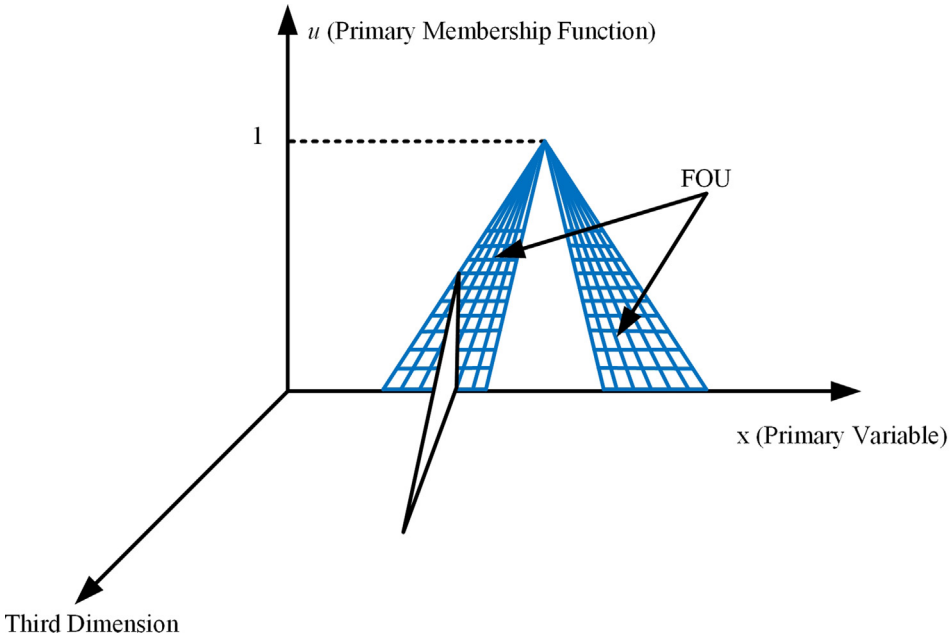

Fig. 5. T2FS Membership Function.

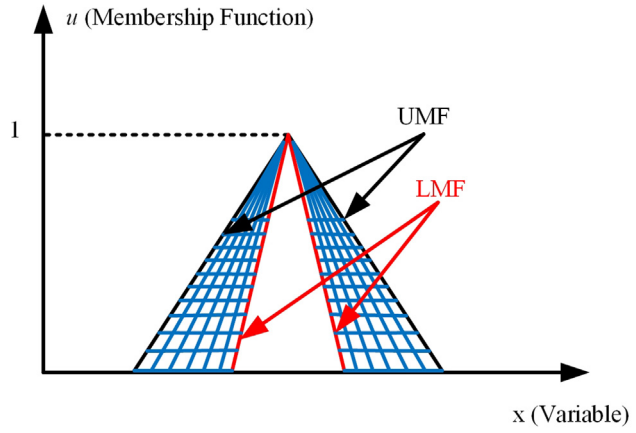

Fig. 6. IT2FS Membership Function.

$$\tilde{\mu}_1 = \left[\bar{\mu}_1, \underset{-1}{\mu}\right], \tilde{\mu}_2 = \left[\bar{\mu}_2, \underset{-2}{\mu}\right] \cdots \tilde{\mu}_n = \left[\bar{\mu}_n, \underset{-n}{\mu}\right] \tag{37}$$

Here, $\bar{\mu}_1 and \underset{-1}{\mu}$ are the membership certainty degrees of the UMF and LMF, respectively. The set of total membership certainties for each rule is defined as Eq. (38).

$$f^j = \left[\bar{f}^j, \underset{-}{f}^j\right] \tag{38}$$

In Eq. (37), $\bar{f}^j and \underset{-}{f}^j$ are defined as Eq. (39) and Eq. (40), respectively.

$$\underset{-}{f}^j = \underset{-1}{\mu}(x_1) \cap \underset{-2}{\mu}(x_2) \cap \cdots \cap \underset{-n}{\mu}(x_n) \tag{39}$$

$$\bar{f}^j = \bar{\mu}_1(x_1) \cap \bar{\mu}_2(x_2) \cap \cdots \cap \bar{\mu}_n(x_n) \tag{40}$$

The result set C_j of the r. rule is an interval set and is defined as in the Eq. (41).

$$C^j = \left[c_l^j, c_r^j\right] \tag{41}$$

The obtained output y_{net} is the net output of T2FS and defined as $y_{net} = [y_l, y_r]$. y_l and y_r can be calculated using a type reduction method. Then, the type-reduced fuzzy set for IT2FS can be expressed as $Y_{TR} = [y_l(x), y_r(x)]$. In this expression, the Y_{TR} is a IT1FS whose two endpoints are y_l and y_r. The output of T2FS can be calculated by using the average values of y_l and y_r with the help of $Y = (y_l + y_r)/2$.

The output set corresponding to each rule of T2FS is a type-2 set. The type reducer combines all these output sets in the same way that a type-1 defuzzifier combines the type-1 rule output sets (Mendel, T2FS: Type Reduction). Then, a center calculation is made on this T2FS, and at the end of this process, a reduced set is obtained that results in the T1FS. Many types of reduction methods have been proposed in the literature. The most widely used type reduction and clarification method is the iterative Karnik and Mendel (KM) algorithm. In this study, the KM method is preferred for type reduction.

Karnik and Mendel Type Reduction Method:

- Calculating y_l consists of five steps.
  i. The c_l^j are sorted in ascending order as $c_l^1 \le c_l^2 \le \cdots \le c_l^N (j = 1, 2, ..., N)$. The corresponding indices of the sorted c_l^j and the appropriate weights of $\underset{-}{f}$ and $\bar{f}$ are equated.
  ii. Initialize f_i and calculate y as in the Eqs. (42) and (43).

$$f_i = \frac{\underset{-i}{f} + \bar{f}_i}{2} \quad i = 1, 2, \cdots, N \tag{42}$$

$$y = \frac{\sum_{i=1}^{N} f_i c_l^i}{\sum_{i=1}^{N} f_i} \tag{43}$$

  iii. The switching point L is found to be $c_l^i \le y \le c_l^{i+1} (1 \le L \le N-1)$
  iv. f_i is set and y' is calculated as in the Eq. (44) and Eq. (43), respectively.

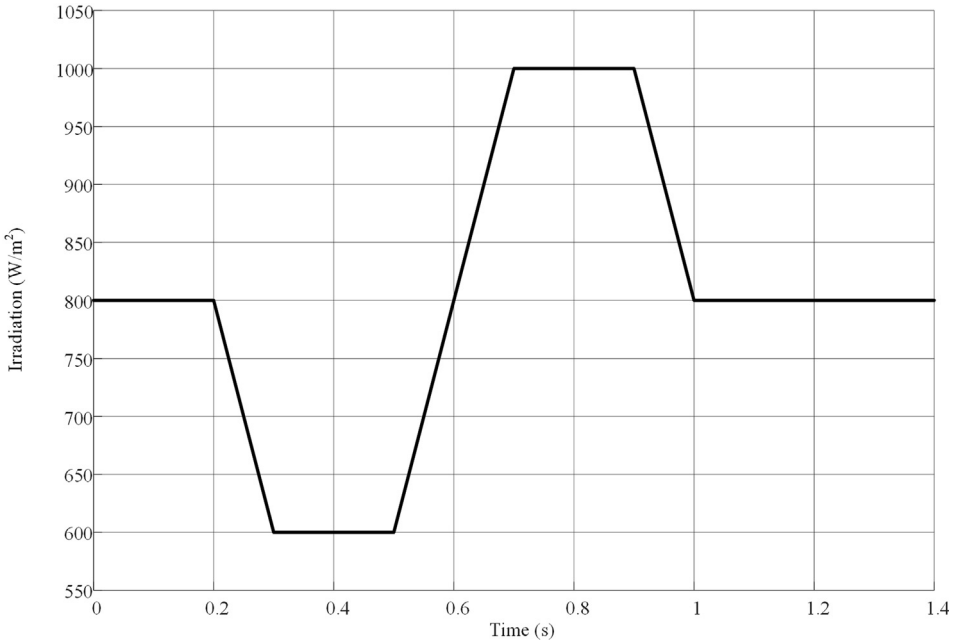

Fig. 7. The variable irradiance profile.

Table 1
The parameters of PV array.

Parameter	Value
Maximum Power (W)	213.15
Cells per Module (N_{cell})	60
Open circuit voltage V_{OC} (V)	36.3
Short circuit current I_{SC} (A)	7.84A
Voltage at MPP V_{MP} (V)	29
Current at MPP I_{MP} (A)	7.35
Temperature (^{O}C)	25
Parallel strings (N_P)	2
Series connected modules per string (N_S)	2

$$x = \begin{cases} \bar{f}^{i} i \le L \\ f^{i} i > L \end{cases} \quad (44)$$

v. The condition $y = y'$ is checked. If not equal go to step 3 and set $y = y'$. Otherwise, it is set directly to $y = y'$.

- Calculating y_r also consists of five steps similarly calculating of y_l.

The proposed mppt system.

The proposed MPPT system is implemented and simulated with using MATLAB/Simulink. Firstly, the variable irradiation profile is prepared as shown in Fig. 7. The irradiance is started with 800 W/m^2, changed and decreased to 600 W/m^2, increased to 1000 W/m^2 and at last, decreased to 800 W/m^2.

Secondly, a used defined PV array is modeled with the parameters which is shown in Table 1. The PV array consists 2 parallel and 2 series connected modules contains 60 cells. The current–voltage and power-voltage characteristics of the proposed PV array under variable irradiance are shown in Fig. 8.

Thirdly, a classical boost dc-dc converter circuit is modelled and connected to the PV array. The parameters of PV panel are chosen from a manual of commercial PV panel. Also, the parameters of boost converter are chosen above the limit values which can be obtained by standard equations [68] for CCM operation. The components of converter and its values are given in Table 2.

Table 2
The components of converter and parameters.

Components and parameters	Value
Input filter capacitor	220 μF
Inductor	2 mH
Forward voltage Vf of IGBT	1 V
Forward voltage Vf of Diode	0.8 V
Output capacitor	470 μF
Resistor (load)	20 Ω
Switching frequency (kHz)	5 kHz

The components of the simulation are combined and also, different MPPT algorithms with SMC, STSMC and STSMC-T2FC methods are modelled and PWM signal is obtained as shown in Fig. 9. Also, the MATLAB/Simulink model of the proposed system is shown in Fig. 10.

Eq. (30) is used for SMC and Eq. (32) is used for STSMC and STSMC-T2FC algorithms. T2FC method is preferred instead of sign (.) function to reduce the chattering problem. And, the effects of T2FC usage are shown in results with graphics and tables. The next step for increasing the performance of MPPT algorithms is to optimize the parameters of control algorithms.

4.3. Optimization of controller parameters

After the simulation environment is created, the optimization of the parameters used in the SMC, STSMC and STSMC-T2FC algorithms is performed by using the MATLAB optimization. The fitness function of optimization algorithms can be chosen as integral absolute error, integral square error, integral time absolute error, inte-

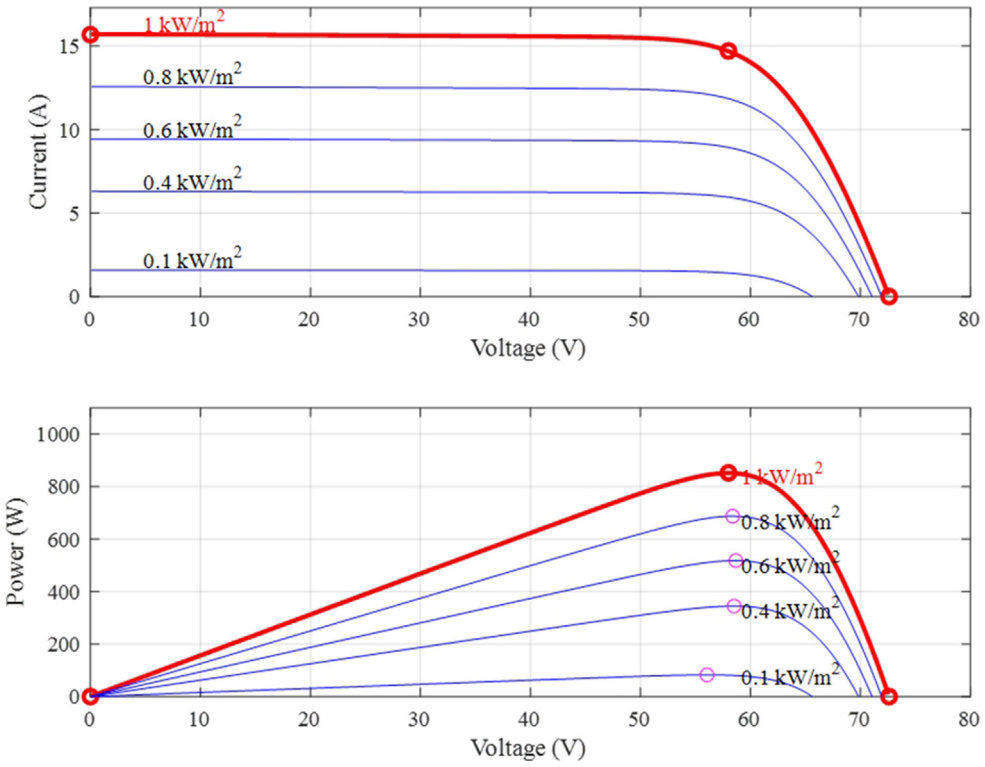

Fig. 8. Current-voltage and power-voltage characteristics of PV array under different irradiances.

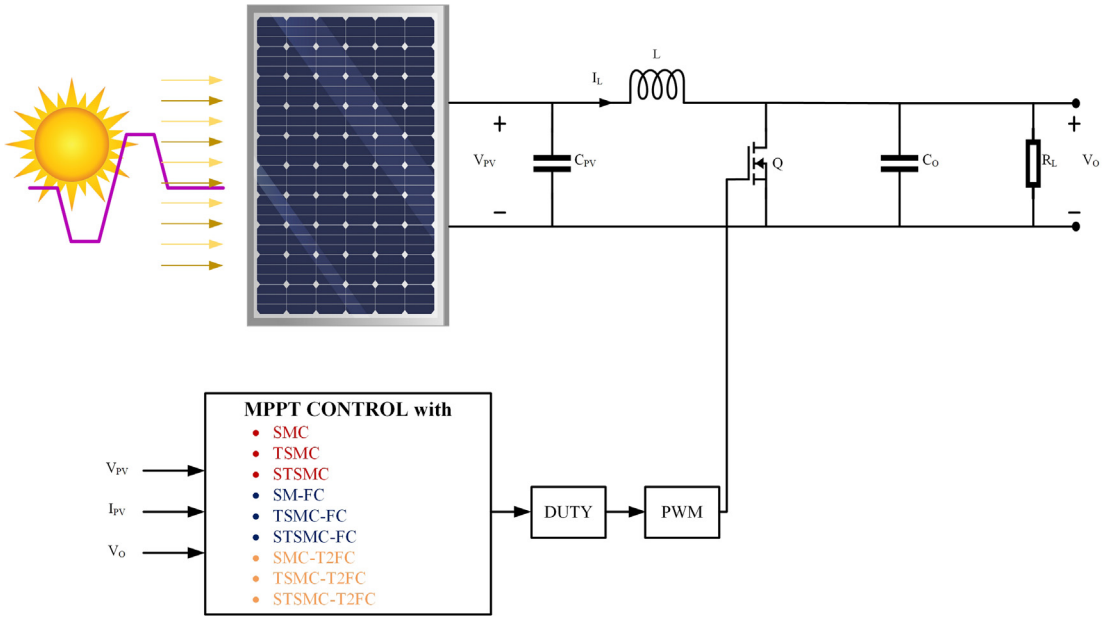

Fig. 9. The proposed MPPT system.

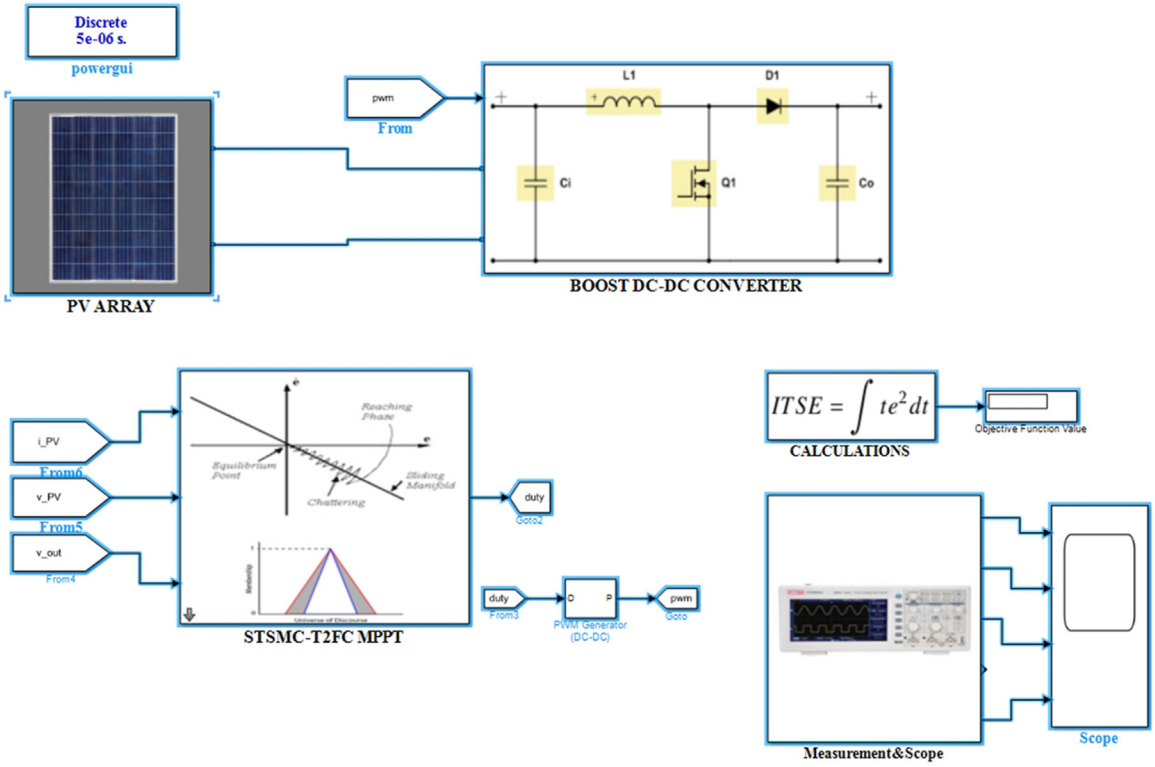

Fig. 10. Simulation model of the proposed system.

gral time square error (ITSE), integral square time error for this purpose. In this study, ITSE is used to tune the parameters and the fitness value is obtained by using Eq. (45). The efficiency of PV (power efficiency) and actual value are compared (P_{PVeff}-P_{PVact} = e_{eff}) and the error is obtained to use for objective function. Output of the objective gives fitness value and it is tried to be reduced below the target value ($i.e. \varepsilon = 10^{-6}$) by bringing it closer to zero, and the minimization function is used for this process. This process and convergence of the error value with optimization toolbox is shown in Fig. 11. As an optimization method, gradient descent (active-set algorithm) is chosen on optimization toolbox. In Table 3, the optimized values of the controllers are given.

$$ITSE = \int te_{eff}^2 dt \tag{45}$$

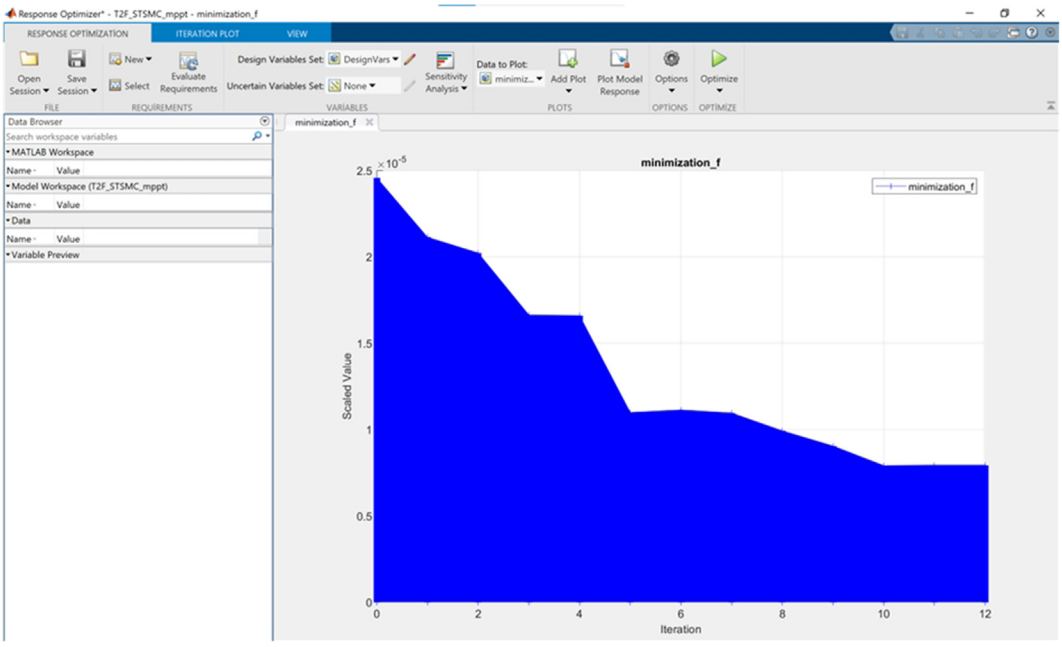

Fig. 11. Convergence graphs of simulation based objective function using gradient descent algorithm with ITSE.

Table 3
The optimized controller parameters of SMC, STSMC and STSMC-T2FC.

The controller parameter	Value
λ_1 (Eq. (32) STSMC and STSMC-T2FC)	0.0110
λ_2 (Eq. (32) STSMC and STSMC-T2FC)	0.00025
λ_3 (Eq. (30) SMC)	0.0724
I_1 (T2FC input gain1)	0.3194
I_2 (T2FC input gain2)	0.3229
O_1 (T2FC output gain)	0.4055

This method is much useful for parameter optimization and it is possible to optimize the parameters online without dealing with solving equations or getting the transfer function of the system.

5. Results

The MPPT system which is fed by a PV panel that modelled with all components. Three different SMC algorithms are proposed for MPPT and the performances of SMC, STSMC and STSMC-T2FC

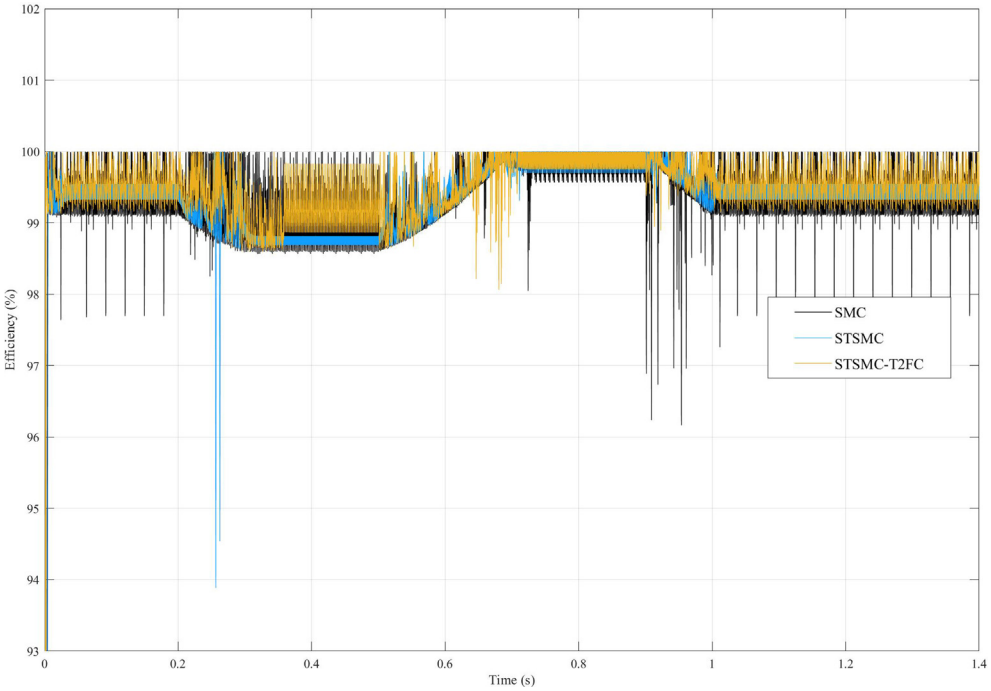

Fig. 12. The efficiency (P_{PV}) of SMC, STSMC and STSMC-T2FC MPPT algorithms.

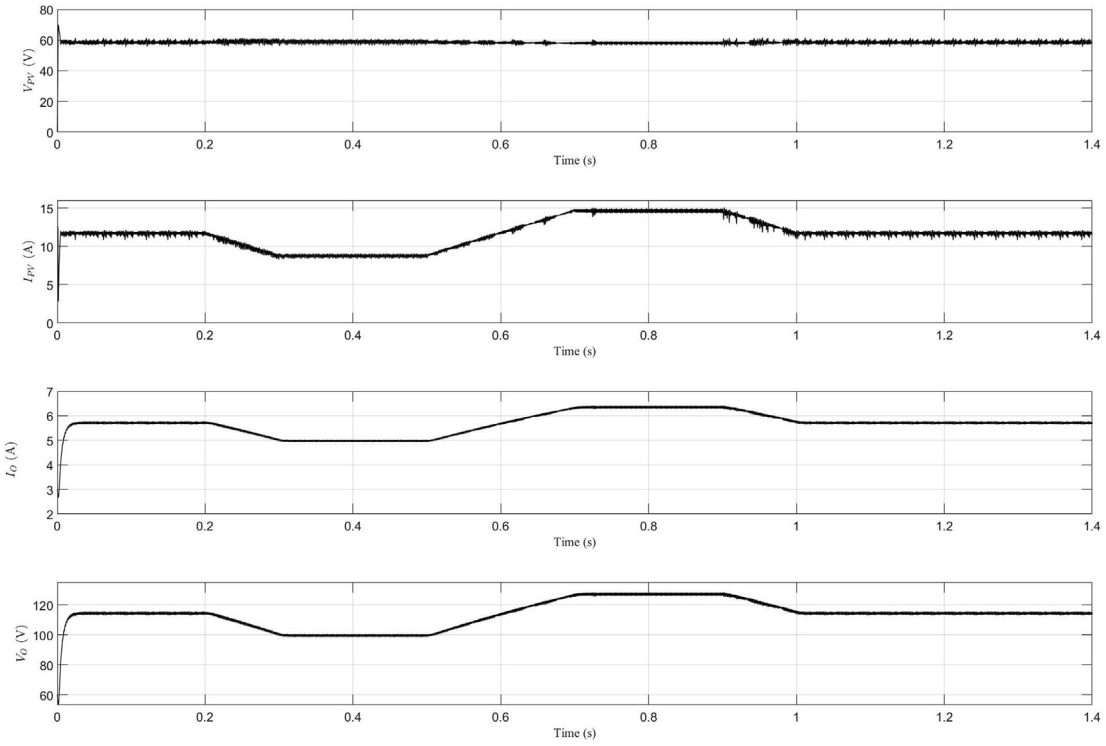

Fig. 13. V_{PV}, I_{PV}, I_O and V_O graphics of SMC MPPT.

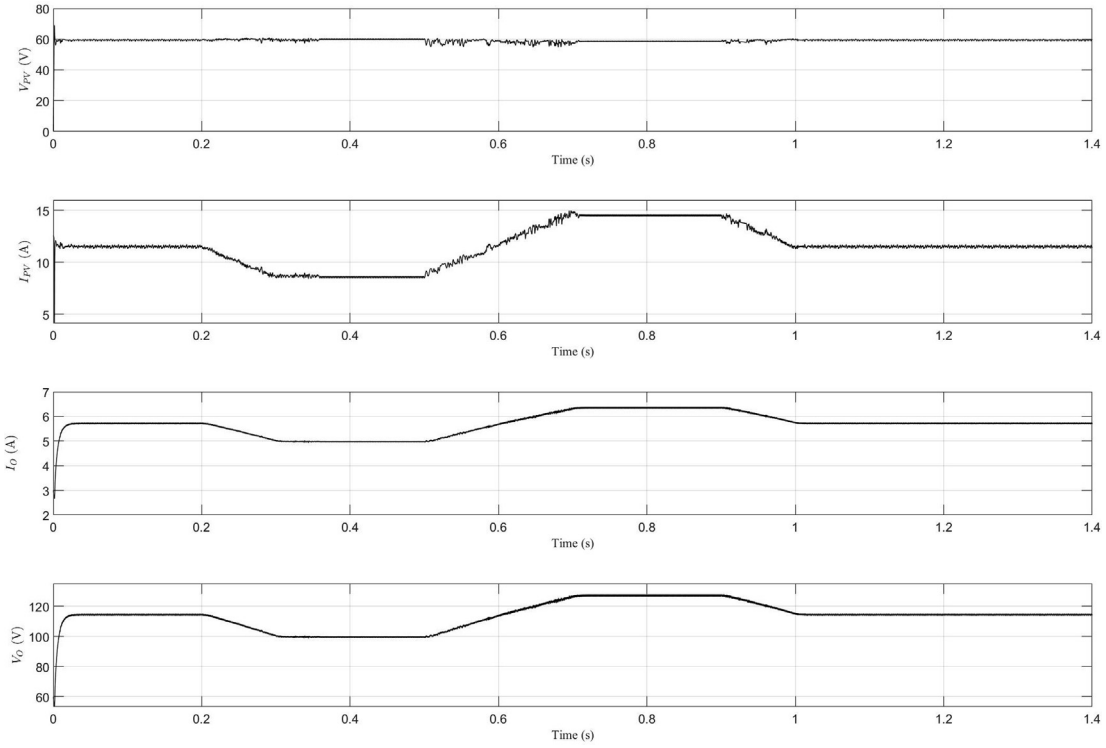

Fig. 14. V_{PV}, I_{PV}, I_O and V_O graphics of STSMC MPPT.

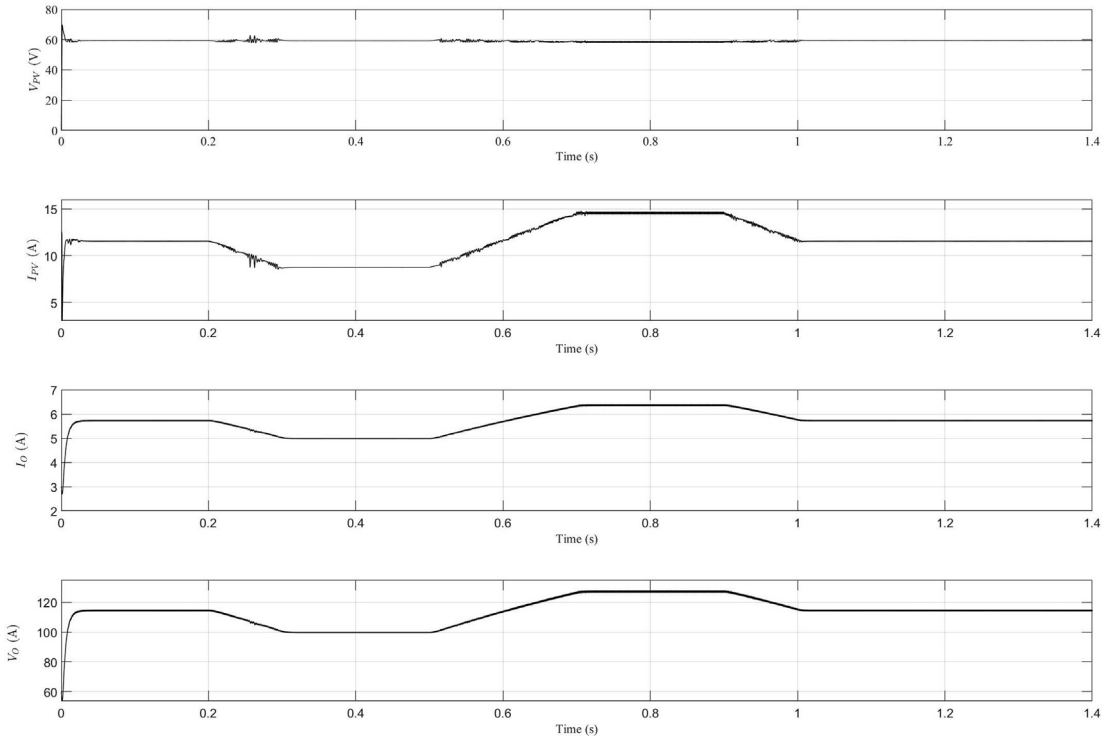

Fig. 15. V_{PV}, I_{PV}, I_O and V_O graphics of STSMC-T2FC MPPT.

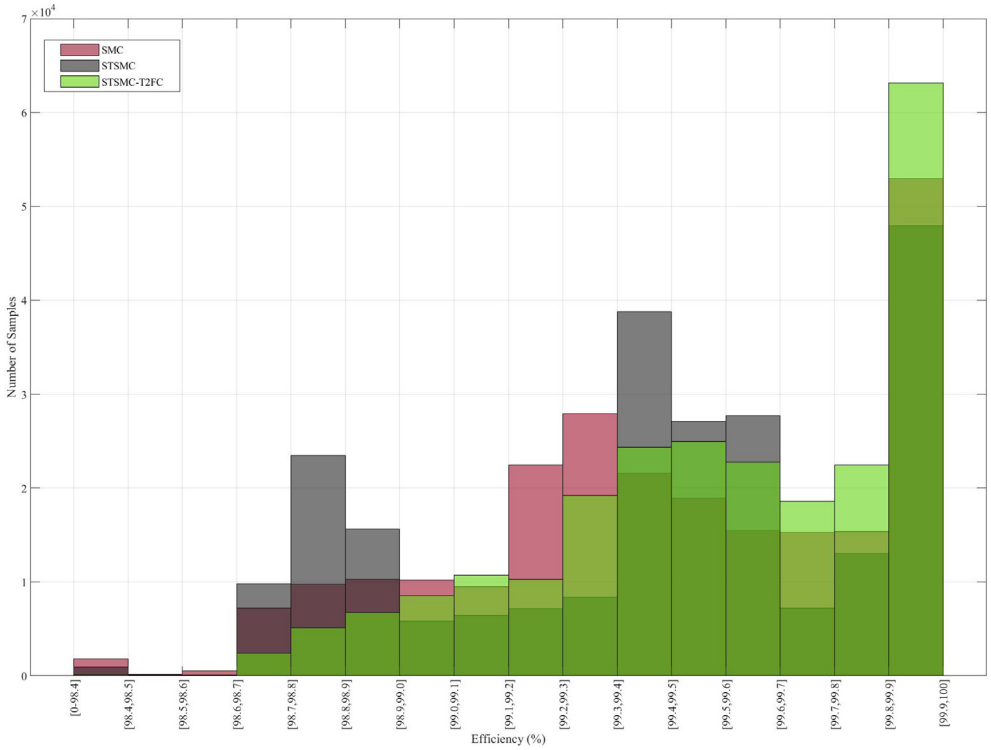

Fig. 16. Histogram for efficiency of SMC, STSMC and STSCM-T2FC MPPT.

Table 4
Performance comparison of the developed methods.

	SMC MPPT	STSMC MPPT	STSMC-T2FC MPPT
Efficiency (Mean)	99.1814 %	99.3335 %	*99.5872 %*
Fluctuation on Efficiency between (Min-Max)	96.1670 %-100 %	93.8861 %-100 %	*98.0615 %-100 %*
Fluctuation on V_{PV} between (Min-Max) Time (0.7sn-0.9sn)	55.473 V-61.750 V 6.227 V (peak to peak)	57.90 V-59.21 V 1.31 V (peak to peak)	*58.2 V-58.88 V* *0.68 V (peak to peak)*
Fluctuation on I_{PV} between (Min-Max) Time (0.7sn-0.9sn)	13.81A-15.065A 1.255A (peak to peak)	14.4A-14.7A 0.3A (peak to peak)	*14.432A-14.62A* *0.188A (peak to peak)*
Fluctuation on V_O between (Min-Max) Time (0.7sn-0.9sn)	125.5 V-128.14 V 2.64 V (peak to peak)	126.48 V-127.98 V 1.5 V (peak to peak)	*126.58 V-127.78 V* *1.2 V (peak to peak)*

methods are compared. Also, the controller parameters are optimized. For these methods, the MPPT efficiency is compared in Fig. 12. Also, V_{PV}, I_{PV}, I_O and V_O variables for SMC, STSMC and STSMC-T2FC MPPT methods are shown in Fig. 13, Fig. 14 and Fig. 15, respectively. It can be seen clearly that chattering and fluctuation with SMC is more than STSMC and STSMC-T2FC MPPT algorithms. With high order structure and fuzzy logic adaptation is decreasing the chattering problem. Additionally, the robustness of the SMC based MPPT methods under variable irradiance can be seen in these figures.

The histogram of Fig. 12 is shown in Fig. 16 that × axis shows efficiency values (%) between 0 % and 100 %, y axis shows the number of samples. It is easy to see that STSMC-T2FC MPPT comes to the fore. Efficiency samples of STSMC-T2FC between (99.9–100 %) are 20 % more than STSMC and 30 % more than SMC. 80 % of the samples of STSMC-T2FC efficiency are in between 99.4 and 100 %.

At last, some parameters are explored and measured to compare the performances of the developed methods. Efficiency (mean of all simulation time), fluctuation on efficiency, V_{PV}, I_{PV}, V_O between (min–max) are presented in Table 4.

6. Conclusion

The important control subject is its robustness under parameter changes and this feature can be proposed for both side parameter changes of converter circuits (changes of input voltage, output voltage and load). For the MPPT application, the most important issue is to make a control that is minimally affected by irradiation change. The decrease in performance due to sensitivity to irradiation changes is the deterioration of controller performance. Especially, SMC method is preferred to improve this situation and to design a robust controller. And then, T2FC algorithm is adapted to the SMC controller in order to minimize the variation in current, voltage and efficiency caused by the current chattering problem of this method. In this study, it is desired to design a robust and highly efficient MPPT algorithm. At this point, some improvements are made based on the SMC method which appears as a robust controller. In order to minimize the chattering problem and increase the robustness, the STSMC algorithm is firstly designed and the FC system is integrated into STSMC. In addition, maximum efficiency is aimed by optimizing the parameters of SMC, STSMC and STSMC-T2FC methods. The MPPT performance of the SMC method was determined more than 99 % in general, and the designed STSMC-T2FC algorithm give good results by greatly reducing the oscillations in voltage, current and efficiency parameters. With 5 kHz switching frequency, all the results are obtained as much satisfactory. The efficiency of SMC MPPT is 99.1814 %, STSMC MPPT is 99.3335 % and STSMC-T2FC MPPT is 99.5872 %. The efficiency performances are very close to each other but STSMC-T2FC provided the best results. And the effects of T2FC adaptation to SMC can be directly seen with the obtained results. The fluctuation on efficiency for SMC MPPT has nearly 4 % band, STSMC MPPT has nearly 6 % band and STSMC-T2FC has nearly<2 % band. Also, fluctuation on V_{PV} for SMC MPPT is 6.227 V, STSMC MPPT is 1.31 V and STSMC-T2FC is 0.68 V (for mean 58.5 V). The fluctuation is decreased to 1.16 % from 10.64 % on V_{PV} values. Additionally, the fluctuation on IPV for SMC MPPT is 1.255A, STSMC MPPT is 0.3A and STSMC-T2FC is 0.188A (for mean 14.5A). The fluctuation is decreased to 1.29 % from 8.65 % on IPV values. The fluctuation on VO of the converter for SMC MPPT is 2.64 V, STSMC MPPT is 1.5 V and STSMC-T2FC MPPT is 1.2 V. The fluctuation is decreased to 0.94 % from 2.07 % on V_O values. These results show that the fluctuation supported from chattering problem are reduced for all these parameters and it shows the efficiency of T2FC adaptation to STSMC.

- All authors have participated in (a) conception and design, or analysis and interpretation of the data; (b) drafting the article or revising it critically for important intellectual content; and (c) approval of the final version.
- This manuscript has not been submitted to, nor is under review at, another journal or other publishing venue.
- The author has no affiliation with any organization with a direct or indirect financial interest in the subject matter discussed in the manuscript
- The following author have affiliation with organizations with direct or indirect financial interest in the subject matter discussed in the manuscript:

Author's name Affiliation.
Korhan Kayisli Gazi University.

Declaration of Competing Interest

The authors declare that they have no known competing financial interests or personal relationships that could have appeared to influence the work reported in this paper.

References

[1] Mamatha G. Perturb and observe MPPT algorithm implementation for PV applications. International Journal of Computer Science and Information Technologies 2015;6(2):1884–7.
[2]] Ibrahim O, Yahaya NZ, Saad N, & Umar MW. Matlab/Simulink model of solar PV array with perturb and observe MPPT for maximising PV array efficiency. In 2015 IEEE conference on energy conversion (CENCON) (pp. 254-258). IEEE. (2015, October).
[3] Killi M, Samanta S. Modified perturb and observe MPPT algorithm for drift avoidance in photovoltaic systems. IEEE Trans Ind Electron 2015;62(9):5549–59.
[4] Ahmed J, Salam Z. An improved perturb and observe (P&O) maximum power point tracking (MPPT) algorithm for higher efficiency. Appl Energy 2015;150:97–108.
[5] Devi VK, Premkumar K, Beevi AB, Ramaiyer S. A modified Perturb & Observe MPPT technique to tackle steady state and rapidly varying atmospheric conditions. Sol Energy 2017;157:419–26.
[6] Belkaid A, Colak I, Kayisli K. A novel approach of perturb and observe technique adapted to rapid change of environmental conditions and load. Electr Power Compon Syst 2020;48(4–5):375–87.
[7] Alik R, Jusoh A. Modified Perturb and Observe (P&O) with checking algorithm under various solar irradiation. Sol Energy 2017;148:128–39.
[8] Belkaid A, Colak I, Kayisli K. Implementation of a modified P&O-MPPT algorithm adapted for varying solar radiation conditions. Electr Eng 2017;99(3):839–46.

[9] Abdel-Salam M, El-Mohandes MT, Goda M. An improved perturb-and-observe based MPPT method for PV systems under varying irradiation levels. Sol Energy 2018;171:547–61.
[10] Chermitti A, Boukli-Hacene O, Mohamed B. Improvement of the“ Perturb and Observe” MPPT Algorithm in a Photovoltaic System under Rapidly Changing Climatic Conditions. International Journal of Computer Applications 2012;56 (12).
[11] John R, Mohammed SS, & Zachariah R. Variable step size Perturb and observe MPPT algorithm for standalone solar photovoltaic system. In: 2017 IEEE International Conference on Intelligent Techniques in Control, Optimization and Signal Processing (INCOS) (pp. 1-6). IEEE. (2017, March).
[12] Ali ZM, Vu Quynh N, Dadfar S, Nakamura H. Variable step size perturb and observe MPPT controller by applying θ-modified krill herd algorithm-sliding mode controller under partially shaded conditions. J Cleaner Prod 2020;271:122243.
[13] Jusoh AB, Mohammed OJEI, Sutikno T. Variable step size Perturb and observe MPPT for PV solar applications. Telkomnika 2015;13(1):1–12. doi: https://doi.org/10.12928/telkomnika.v13i1.1180.
[14] Saidi K, Maamoun M, Bounekhla MH. A new high performance variable step size perturb-and-observe MPPT algorithm for photovoltaic system. International Journal of Power Electronics and Drive Systems 2019;10 (3):1662–74.
[15] Benhadouga S, Belkaid A, Colak I, Meddad M, & Eddiai A. Experimental Validation of The Sliding Mode Controller to Improve The Efficiency of The MPPT Solar System. In: 2021 10th International Conference on Renewable Energy Research and Application (ICRERA) (pp. 333-337). IEEE. (2021, September).
[16] Bianconi E, Calvente J, Giral R, Mamarelis E, Petrone G, Ramos-Paja CA, et al. Perturb and observe MPPT algorithm with a current controller based on the sliding mode. Int J Electr Power Energy Syst 2013;44(1):346–56.
[17] Mohanty S, Subudhi B, Ray PK. A grey wolf-assisted perturb & observe MPPT algorithm for a PV system. IEEE Trans Energy Convers 2016;32(1):340–7.
[18] Sundareswaran K, Vignesh kumar V, Palani S. Application of a combined particle swarm optimization and perturb and observe method for MPPT in PV systems under partial shading conditions. Renewable Energy 2015;75:308–17.
[19] Koad RB, Zobaa AF, El-Shahat A. A novel MPPT algorithm based on particle swarm optimization for photovoltaic systems. IEEE Trans Sustainable Energy 2016;8(2):468–76.
[20] Kamal NA, Azar AT, Elbasuony GS, Almustafa KM, & Almakhles D. PSO-based adaptive perturb and observe MPPT technique for photovoltaic systems. In: International Conference on Advanced Intelligent Systems and Informatics (pp. 125-135). Springer, Cham. (2019, October).
[21] Celikel R, Yilmaz M, Gundogdu A. A voltage scanning-based MPPT method for PV power systems under complex partial shading conditions. Renewable Energy 2022;184:361–73.
[22] Sera D, Mathe L, Kerekes T, Spataru SV, Teodorescu R. On the perturb-and-observe and incremental conductance MPPT methods for PV systems. IEEE J Photovoltaics 2013;3(3):1070–8.
[23] Banu IV, Beniugă R, Istrate M. Comparative analysis of the perturb-and-observe and incremental conductance MPPT methods. In: 2013 8Th International Symposium on advanced topics in electrical engineering (ATEE). IEEE; 2013, May. p. 1–4.
[24] Khadidja S, Mountassar M, & M'hamed B. Comparative study of incremental conductance and perturb & observe MPPT methods for photovoltaic system. In: 2017 International Conference on Green Energy Conversion Systems (GECS) (pp. 1-6). IEEE. (2017, March).
[25] Christopher IW, Ramesh R. Comparative study of P&O and InC MPPT algorithms. American Journal of Engineering Research (AJER) 2013;2 (12):402–8.
[26] Jain K, Gupta M, & Bohre AK. Implementation and comparative analysis of P&O and INC MPPT method for PV system. In: 2018 8th IEEE India International Conference on Power Electronics (IICPE) (pp. 1-6). IEEE. (2018, December).
[27] Harini K, & Syama S. Simulation and analysis of incremental conductance and Perturb and Observe MPPT with DC-DC converter topology for PV array. In: 2015 IEEE International Conference on Electrical, Computer and Communication Technologies (ICECCT) (pp. 1-5). IEEE. (2015, March).
[28] El Gouri R, Brahim M, Hlou L. A Comparative Study Of Mppt Technical Based On Fuzzy Logic And Perturb Observe Algorithms For Photovoltaic Systems. Journal of Theoretical & Applied Information Technology 2013;58 (2):336–46.
[29] Abdelwahab SAM, Hamada AM, Abdellatif WS. Comparative analysis of the modified perturb & observe with different MPPT techniques for PV grid connected systems. International journal of renewable energy Research 2020;10(1):55–164.
[30] Rahman MW, Bathina C, Karthikeyan V, & Prasanth R. Comparative analysis of developed incremental conductance (IC) and perturb & observe (P&O) MPPT algorithm for photovoltaic applications. In: 2016 10th International Conference on Intelligent Systems and Control (ISCO) (pp. 1-6). IEEE. (2016, January).
[31] Selman NH, Mahmood JR. Comparison between perturb & observe, incremental conductance and fuzzy logic MPPT techniques at different weather conditions. International Journal of Innovative Research in Science, Engineering and Technology 2016;5(7):12556–69.
[32] Jha K, & Dahiya R. Comparative study of perturb & observe (P&O) and incremental conductance (IC) MPPT technique of PV system. In: Numerical Optimization in Engineering and Sciences (pp. 191-199). Springer, Singapore. (2020).
[33] Belkaid A, Colak I, & Kayisli K. A comprehensive study of different photovoltaic peak power tracking methods. In: 2017 IEEE 6th International Conference on Renewable Energy Research and Applications (ICRERA) (pp. 1073-1079). IEEE. (2017, November).
[34] Balal A, Murshed M. Implementation and comparison of Perturb and Observe, and Fuzzy Logic Control on Maximum Power Point Tracking (MPPT) for a Small Satellite. Journal of Soft Computing and Decision Support Systems 2021;8 (2):14–8.
[35] Otmane H, Mouloudi Y, Mokhtar B. Comparative analysis of cascaded Fuzzy-PI controllers based-MPPT and perturb and observe MPPT in a grid-connected PV system operating under different weather and loading conditions. International Journal of Power Electronics and Drive Systems 2019;10 (4):1986–94.
[36] Remoaldo D, Jesus I. Analysis of a traditional and a fuzzy logic enhanced perturb and observe algorithm for the MPPT of a photovoltaic system. Algorithms 2021;14(1):24.
[37] Belkaid A, Colak I, Kayisli K, & Bayindir R. Improving PV system performance using high efficiency fuzzy logic control. In: 2020 8th International Conference on Smart Grid (icSmartGrid) (pp. 152-156). IEEE. (2020, June).
[38] Haji D, & Genc N. Fuzzy and P&O based MPPT controllers under different conditions. In: 2018 7th International Conference on Renewable Energy Research and Applications (ICRERA) (pp. 649-655). IEEE. (2018, October).
[39] Chtouki I, Wira P, Zazi M, Collicchio B, Meddour S. Design, implementation and comparison of several neural perturb and observe MPPT methods for photovoltaic systems. International Journal of Renewable Energy Research (IJRER) 2019;9(2):757–70.
[40] Rezvani A, Izadbakhsh M, Gandomkar M, Vafaei S. Investigation of ANN-GA and modified perturb and observe MPPT techniques for photovoltaic system in the grid connected mode. Indian Journal of Science and Technology 2015;8 (1):87–95.
[41] Murtaza AF, Sher HA, Chiaberge M, Boero D, De Giuseppe M, & Addoweesh KE. A novel hybrid MPPT technique for solar PV applications using perturb & observe and fractional open circuit voltage techniques. In Proceedings of 15th International Conference MECHATRONIKA (pp. 1-8). IEEE. (2012, December).
[42] Atallah AM, Abdelaziz AY, Jumaah RS. Implementation of perturb and observe MPPT of PV system with direct control method using buck and buck-boost converters. Emerging Trends in Electrical, Electronics & Instrumentation Engineering: An international Journal (EEIEJ) 2014;1(1):31–44.
[43] Sahu TP, Dixit TV, Kumar R. Simulation and analysis of perturb and observe MPPT algorithm for PV array using ĊUK converter. Advance in Electronic and Electric Engineering 2014;4(2):213–24.
[44] Sahu TP, & Dixit TV. Modelling and analysis of Perturb & Observe and Incremental Conductance MPPT algorithm for PV array using Ċuk converter. In: 2014 IEEE Students' Conference on Electrical, Electronics and Computer Science (pp. 1-6). IEEE. (2014, March).
[45] Belkaid A, Colak I, Kayisli K, Bayindir R. Design and implementation of a cuk converter controlled by a direct duty cycle INC-MPPT in PV battery system. International Journal of Smart Grid-ijSmartGrid 2019;3(1):19–25.
[46] González I, Salazar S, Lozano R. Chattering-free sliding mode altitude control for a quad-rotor aircraft: Real-time application. J Intell Rob Syst 2014;73 (1):137–55.
[47] Xu Y. Chattering free robust control for nonlinear systems. IEEE Trans Control Syst Technol 2008;16(6):1352–9.
[48] Kayisli K, Tuncer S, Poyraz M. A Novel Power Factor Correction System Based on Sliding Mode Fuzzy Control. Electr Power Compon Syst 2017;45(4):430–41.
[49] Akpolat HZ, Asher GM, Clare JC. A practical approach to the design of robust speed controllers for machine drives. IEEE Trans Ind Electron 2000;47 (2):315–24.
[50] Shannan NMAA, Yahaya NZ, & Singh B. Single-diode model and two-diode model of PV modules: A comparison. In: 2013 IEEE international conference on control system, computing and engineering (pp. 210-214). IEEE. (2013, November).
[51] Nema S, Nema RK, Agnihotri G. Matlab/simulink based study of photovoltaic cells/modules/array and their experimental verification. Int J Energy Environ 2010;1(3):487–500.
[52] Kchaou A, Naamane A, Koubaa Y, M'sirdi N. Second order sliding mode-based MPPT control for photovoltaic applications. Sol Energy 2017;155:758–69.
[53] Belkaid A, Gaubert JP, Gherbi A. An improved sliding mode control for maximum power point tracking in photovoltaic systems. Journal of Control Engineering and Applied Informatics 2016;18(1):86–94.
[54] Akpolat ZH. Non-singleton fuzzy logic control of a dc motor. Journal of Applied Sciences 2005;5(5):887–91.
[55] Ozek MB, Akpolat ZH. A software tool: Type-2 fuzzy logic toolbox. Computer Applications in Engineering Education 2008;16(2):137–46.
[56] Özek MB, Akpolat ZH. Bulanık mantık için yeni bir yaklaşım: Tip-2 bulanık mantık. Eng Sci 2010;5(3):541–57.
[57] Aliasghary M, Eksin I, Guzelkaya M, Kumbasar T. General derivation and analysis for input–output relations in interval type-2 fuzzy logic systems. Soft Comput 2015;19(5):1283–93.
[58] Öztürk C. “Learning of interval type-2 fuzzy logic systems using big bang–big crunch optimization”, pHd Thesis, Istanbul Technical University, Graduate School of Natural and Applied Sciences, 2014.

[59] Liang Q, Mendel JM. Interval type-2 fuzzy logic systems: Theory and design. IEEE Trans Fuzzy Syst 2000;8(5):535–50.
[60] Soliman MA, Al-Durra A, Hasanien HM. Electrical parameters identification of three-diode photovoltaic model based on equilibrium optimizer algorithm. IEEE Access 2021;9:41891–901.
[61] Selem SI, El-Fergany AA, Hasanien HM. Artificial electric field algorithm to extract nine parameters of triple-diode photovoltaic model. Int J Energy Res 2021;45(1):590–604.
[62] Qais MH, Hasanien HM, Alghuwainem S. Transient search optimization for electrical parameters estimation of photovoltaic module based on datasheet values. Energy Convers Manage 2020;214:112904.
[63] Qais MH, Hasanien HM, Alghuwainem S. Parameters extraction of three-diode photovoltaic model using computation and Harris Hawks optimization. Energy 2020;195:117040.
[64] Elazab OS, Debouza M, Hasanien HM, Muyeen SM, Al-Durra A. Salp swarm algorithm-based optimal control scheme for LVRT capability improvement of grid-connected photovoltaic power plants: design and experimental validation. IET Renew Power Gener 2020;14(4):591–9.
[65] Fei J, Wang H, Fang Y. Novel neural network fractional-order sliding-mode control with application to active power filter. IEEE Transactions on Systems, Man, and Cybernetics: Systems 2021;52(6):3508–18.
[66] Fei J, Chen Y, Liu L, Fang Y. "Fuzzy multiple hidden layer recurrent neural control of nonlinear system using terminal sliding-mode controller". IEEE transactions on cybernetics (early access), pp. 1-16, 2021.
[67] Wang Z, Fei J. Fractional-order terminal sliding mode control using self-evolving recurrent Chebyshev fuzzy neural network for MEMS gyroscope. IEEE Trans Fuzzy Syst 2022;30(7):2747–58.
[68] Kayisli K, Tuncer S, Poyraz M. An educational tool for fundamental DC–DC converter circuits and active power factor correction applications. Computer Applications in Engineering Education 2013;21(1):113–34.

Dr.Korhan Kayisli received a BSc degree in electronics education from Sakarya University, Sakarya, Turkey, in 2001, and an MSc degree in Electronics and Computer Science from Firat University, Elazig, Turkey, in 2004. He received PhD degree at the area of power electronics in Electric and Electronics Engineering at Firat University, Elazig, Turkey, in 2012. He worked as a research assistant between 2002 and 2012. He has worked in Firat University, Bitlis Eren University, Gelisim University, Nisantasi University, respectively. He is currently an assistant professor in the Department of Electrical Electronics Engineering, Engineering Faculty, Gazi University, Ankara, Turkey. He is the co-editor of International Journal of Renewable Energy Research and International Journal of Engineering Science and Application. He also served as reviewer to many high ranked scientific journals. His fields of interest are power electronics, converter circuits, power factor correction, robust control, and renewable energy systems. He has published many journal and conference papers on these areas. Additionally, he has worked as researcher in two EU mobility projects and other some projects.